Pharmaceutical Research, Vol. 25, No. 10, October 2008 (© 2008)
DOI: 10.1007/s11095-008-9637-9

Research Paper

Rate-Limiting Steps of Oral Absorption for Poorly Water-Soluble Drugs in Dogs; Prediction from a Miniscale Dissolution Test and a Physiologically-Based Computer Simulation

Ryusuke Takano,[1,4] Kentaro Furumoto,[1] Koji Shiraki,[1] Noriyuki Takata,[1] Yoshiki Hayashi,[2] Yoshinori Aso,[2] and Shinji Yamashita[3]

Received March 26, 2008; accepted May 21, 2008; published online June 17, 2008

Purpose. Nonlinear oral absorption due to poor solubility often impedes drug development. The purpose of this study was to elucidate the rate-limiting process in oral absorption of Biopharmaceutical Classification System (BCS) class II (low solubility–high permeability) drugs in order to predict nonlinear absorption of dose caused by solubility-limited absorption.
Methods. Oral absorption of danazol, griseofulvin, and aprepitant was predicted from a miniscale dissolution test and a physiologically-based model. The effect of particle size reduction and dose increase on absorption was investigated *in vitro* and *in vivo* to clarify the rate-limiting steps of dissolution-rate-limited and solubility-limited absorption.
Results. The rate-limiting steps of oral absorption were simulated and increase in the dissolution rate and administration dose showed a shift from dissolution rate-limited to solubility-limited absorption. In the study in dogs, particle size reduction improved the oral absorption of large particle drugs but had little effect on small particle drugs. Dose nonlinearity was observed with small particles at a high dose. Our model quantitatively predicted results observed *in vivo*, including but not exclusively, dissolution-rate-limited and solubility-limited absorption.
Conclusion. The present study provides a powerful tool to predict dose nonlinearity and will aid in the success of BCS class II drug development.

KEY WORDS: dissolution; *in vitro–in vivo* correlation; oral absorption; poorly water-soluble; rate-limiting step.

INTRODUCTION

The number of poorly water-soluble drug candidates in drug discovery has recently increased (1). Their limited solubility often causes poor and variable oral absorption because the dissolution rate or solubility is insufficient to completely dissolve the drug in the gastrointestinal (GI) tract. Low solubility might lead to nonlinear dose-dependent oral absorption; that is, the fraction of dose absorbed (F_a) decreases as dose increases. In preclinical studies, variable and nonlinear absorption from low solubility makes it difficult to evaluate the safety of a drug. Moreover, the efficacy and therapeutic window of a drug might be underestimated and, thus, the probability of successful development is diminished. Therefore, it is critical to predict nonlinear absorption of a candidate compound at the drug discovery stage.

Dissolution in the GI tract may have a great impact on the oral absorption of Biopharmaceutical Classification System (BCS) class II (low soluble-high permeable as defined by the Food and Drug Administration) drugs. Oral absorption for this class of drugs has been categorized into two types, dissolution rate-limited and solubility-limited, based on the solubility, dissolution rate, and permeability of a drug (2,3). Drug dissolution in the GI tract *in vivo* occurs under sink conditions and, if the drug dissolution rate is slower than the permeation rate through the intestinal membrane, oral absorption of a drug may be limited by the dissolution rate. In the case of dissolution-rate-limited absorption, the amount of drug absorbed shows a linear relation to dose and particle size reduction increases absorption. On the other hand, if the dose-to-solubility ratio is high and/or the dissolution rate is far greater than the permeation rate, the absorption of a drug is limited not only by the dissolution rate but also by the saturated solubility. In the case of solubility-limited absorption, dissolution occurs under nonsink conditions and, thus, increases in the dissolution rate or the administration dose do not lead to an increase in either the dissolved or absorbed amount in the GI tract. The amount of drug absorbed reaches saturation with a high dose regimen. In addition, particle size reduction does not increase the amount absorbed. Therefore, if the oral absorption is solubility-limited, it is difficult to improve the exposure of a drug either by increasing dose or by reducing particle size.

Oral absorption of drugs from solid dosage forms is determined by the dissolution rate, solubility, and intestinal mem-

[1] Discovery Platform Technology Department, Chugai Pharmaceutical Co., Ltd., 1-135 Komakado, Gotemba, Shizuoka, 412-8513, Japan.
[2] Pre-clinical Research Department, Chugai Pharmaceutical Co., Ltd., 1-135 Komakado, Gotemba, Shizuoka, 412-8513, Japan.
[3] Faculty of Pharmaceutical Sciences, Setsunan University, 45-1 Nagaotoge-cho, Hirakata, Osaka, 573-0101, Japan.
[4] To whom correspondence should be addressed. (e-mail: takanorus@chugai-pharm.co.jp)

brane permeability (4,5). We have developed a prediction system for oral absorption of BCS Class II drugs using the dissolution rate and solubility determined *in vitro* in physiologically-based models (6). In this system, the amount of drug absorbed in the intestinal tract is simulated using dissolution rate, saturated solubility, permeation rate, and the dose administered. The rate limiting process *in vivo* can be deduced from the simulated concentration of drug in the intestine during absorption, which is valid whether the dissolution occurs under sink or nonsink conditions.

In the present study, the rate-limiting steps of oral absorption for three BCS class II drugs—danazol, griseofulvin and aprepitant—were analyzed both *in vitro* and *in vivo*. Several sizes of particles of drugs having various dissolution rates were prepared to investigate the effect of particle size reduction on absorption. Oral absorption at several doses of solid particles was simulated using a miniscale dissolution test and a physiologically-based model. Concurrently, an oral absorption study in dogs was carried out using the model drugs to compare observed results with the predicted data.

THEORY

The fraction dose absorbed (F_a) of poorly water-soluble drugs was simulated theoretically from dissolution and permeation parameters (6).

Extraction of the Dissolution Parameter *z* from an *In Vitro* Dissolution Curve

The Noyes–Whitney model was used to describe the dissolution of the solid drugs (7). To simulate drug dissolution *in vivo* from the *in vitro* dissolution profile in a miniscale dissolution test, we first defined parameter z, a hybrid parameter determined from the formula $3D/\rho hr_0$, where D is the diffusion coefficient, ρ is the density of drug, h is the diffusion layer thickness, and r_0 is the initial particle radius. The z values were estimated from the *in vitro* data from Eq. 1, using mathematical software SAAM II version 1.2 (SAAM Institute Inc., University of Washington, WA, USA).

$$\frac{dX_{d,vitro}(t)}{dt} = \frac{3D}{\rho hr_0} \times X_{0,s,vitro} \times \left(\frac{X_{s,vitro}(t)}{X_{0,s,vitro}}\right)^{2/3} \times \left(C_s - \frac{X_{d,vitro}(t)}{V_{vitro}}\right)$$
$$= z \times X_{0,s,vitro} \times \left(X_{s,vitro} \times \left(\frac{X_{s,vitro}(t)}{X_{0,s,vitro}}\right)^{2/3} \times \left(C_s - \frac{X_{d,vitro}(t)}{V_{vitro}}\right)\right) \quad (1)$$

where $X_{d,vitro}(t)$ is the mass of the dissolved drug at time t, $X_{0,s,vitro}$ is the initial mass of the solid drug, $X_{s,vitro}(t)$ is the mass of the solid drug at time t, C_s is the saturated solubility of the drug, and V_{vitro} is the volume of the dissolution medium.

Calculation of Unstirred Water Layer Permeability

Diffusion through the unstirred water layer (UWL), which is adjacent to the intestinal epithelial membrane, limits the intestinal permeation of highly permeable drugs (8–13). Because UWL permeation can be modeled as a simple diffusion process in a water layer, UWL permeability (P_{UWL}) is represented by the diffusion coefficient and the thickness (δ) of UWL (14) following the Stokes–Einstein equation for small, spherical molecules:

$$P_{UWL} = \frac{D}{\delta} = \frac{k_B T}{6\pi\eta\delta} \times \frac{1}{R} \quad (2)$$

where k_B is the Boltzmann constant, T is the temperature in Kelvin, η is the viscosity of UWL, and R is the molecular radius. Using the effective intestinal membrane permeability of glucose in dogs (16×10^{-4} cm/s) (15), the permeation of which is rate-limited by UWL, the thickness of the diffusion layer of UWL is expressed by Eq. 3 below (6). Molecular radius is a function of the cube root of the molecular weight ($MW^{1/3}$), assuming a spherical molecule, and so the diffusion coefficient can also be expressed using MW. The MW of glucose is 180.

$$\delta = \frac{k_B T}{6\pi\eta} \times \frac{1}{\left(\frac{3}{4\pi\rho} \times MW\right)^{1/3}} \times \frac{1}{P_{UWL}}$$
$$= \frac{k_B T}{6\pi\eta} \times \frac{1}{\left(\frac{3}{4\pi\rho} \times 180\right)^{1/3}} \times \frac{1}{16 \times 10^{-4}} \quad (3)$$

The P_{UWL} for each drug is given by the following equation.

$$P_{UWL} = 16 \times 10^{-4} \times \left(\frac{180}{MW}\right)^{1/3} \quad (4)$$

Simulation of Drug Absorption in Dog Small Intestine

The model for the dissolution and passive permeation of a drug in the small intestine assumes (1) the drug dissolves in the small intestine, not in the stomach or colon; (2) the diffusion layer models the dissolution process; (3) the drug is absorbed in the small intestine, not in the stomach or colon; (4) membrane permeability of a lipophilic drug is high and therefore limited by diffusion through the UWL; (5) the intestinal transit time is 2 h in dogs (16); (6) the intestinal fluid volume V_{vivo} is the volume of water (4 mL/kg) administered to the dogs in the present study; and (7) the effective intestinal surface area S in dog (4 cm^2/kg) is almost one-third that in human (11 cm^2/kg) (2), consistent with the anatomical ratio of dog to human. According to Kararli's report, the small intestine is 225–290 cm long with a diameter of 1 cm in Beagle dogs and is on average 625 cm with a 5-cm diameter in humans (17). Using these values, the entire intestinal surface area relative to body weight in dogs (16–20 π cm^2/ kg) is calculated to be two to three times smaller than that of humans (45 π cm^2/kg). Mass balances of solid and of dissolved drugs in the GI tract are given by the following equations:

$$\frac{dX_{s,vivo}(t)}{dt} = -z \times X_{0,s,vivo} \times \left(\frac{X_{s,vivo}(t)}{X_{0,s,vivo}}\right)^{2/3} \times \left(C_s - \frac{X_{d,vivo}(t)}{V_{vivo}}\right) \quad (5)$$

$$\frac{dX_{d,vivo}(t)}{dt} = z \times X_{0,s,vivo} \times \left(\frac{X_{s,vivo}(t)}{X_{0,s,vivo}}\right)^{2/3} \times \left(C_s - \frac{X_{d,vivo}(t)}{V_{vivo}}\right) \quad (6)$$
$$- P_{UWL} \times S \times \frac{X_{d,vivo}(t)}{V_{vivo}}$$

where $X_{s,vivo}(t)$ is the mass of solid drug in the small intestine at time t and $X_{d,vivo}(t)$ is the mass of dissolved drug in the small intestine at time t. $X_{0,s,vivo}$, which is a function of the number of particles *in vivo*, was set equal to the dose administered. Values for z and C_s obtained from *in vitro* tests were used. The rate of absorption is given by:

$$\frac{dX_{a,vivo}(t)}{dt} = P_{UWL} \times S \times \frac{X_{d,vivo}(t)}{V_{vivo}} \quad (7)$$

where $X_{a,vivo}(t)$ is the mass of absorbed drug at time t.

The predicted fraction of the dose absorbed (F_a) is the ratio between $X_{0,s,vivo}$ and $X_{a,vivo}(t)$ at 2 h.

$$F_a(t) = \frac{X_{a,vivo}(t)}{X_{0,s,vivo}} \times 100 \quad (8)$$

To obtain simulated profiles, the Runge–Kutta method was used with STELLA®5.1.1 software (Cognitus Ltd., North Yorkshire, UK).

Estimation of Rate-Limiting Steps of Oral Absorption

$C_{ratio}(t)$ is the ratio of the intestinal drug concentration at time t to the drug saturated solubility in the simulation of drug absorption, shown here as a percentage.

$$C_{ratio}(t) = \frac{\left(\frac{X_{d,vivo}(t)}{V_{vivo}}\right)}{C_s} \times 100 \quad (9)$$

The concentration gradient across the diffusion layer of the solid surface (h) in Eqs. 5 and 6, which represents $[C_s - (X_{d,vivo}(t)/V_{vivo})]/h$, controls dissolution over time. If $C_{ratio}(t)$ is low ($C_s >> X_{d,vivo}(t)/V_{vivo}$), the drug dissolves under sink conditions. In this case, the oral absorption could be dissolution rate-limited. As $C_{ratio}(t)$ increases, drug dissolution decreases due to the limitation of its solubility (non-sink conditions).

Drug Selection

Danazol, griseofulvin, and aprepitant were selected as the models for poorly water-soluble drugs Table I. The oral absorption of neutral drugs such as danazol and griseofulvin largely depends on dissolution in the small intestine because neutral drugs mainly dissolve in the small intestine, not in the stomach or colon, due to the presence of bile salts. Aprepitant, a free weak base (pKa 4.38), will likely dissolve not only in the small intestine but also in the stomach due to the low gastric pH; however, when the gastric pH is elevated, aprepitant will dissolve mainly in the small intestine and not in the stomach because of the presence of bile salts. In the present study, aprepitant was administered after the dogs had received the gastric acid blocker famotidine and therefore dissolved mainly in the small intestine. Because the present prediction system assumes that drug dissolution and absorption occur in the small intestine, and not in the stomach or colon, the drugs selected were adequate models for establishing an *in vitro–in vivo* correlation.

Collection of Dog Oral Absorption Data

To confirm the rationality of the present system, the value of F_a in dogs was required. Here we utilized the relative bioavailability of a solid dosage form and a solution orally administered (rel. $BA_{solid/solution}$), as an alternative to F_a. The rel. $BA_{solid/solution}$ for lipophilic drugs is almost equal to the F_a of the solid dosage form ($F_{a,solid}$). The relative BA was calculated as the ratio of the area under the curve for solid dosages (AUC_{solid}) to solution dosages ($AUC_{solution}$) where AUC_{solid} is the product of $F_{a,solid}$, $F_{g,solid}$, and $F_{h,solid}$ and $AUC_{solution}$ is the product of $F_{a,solution}$, $F_{g,solution}$, and $F_{h,solution}$ (subscript notation includes administration form). F_g and F_h are the fraction of the dose-escaping metabolism by the GI mucosa and by the liver, respectively.

$$rel.BA_{solid/solution} = \frac{AUC_{solid}}{AUC_{solution}} \times 100 = \frac{F_{a,solid} \times F_{g,solid} \times F_{h,solid}}{F_{a,solution} \times F_{g,solution} \times F_{h,solution}} \times 100 \quad (10)$$

Assuming linear kinetics of drug metabolism from either administration, the relative bioavailability represents the ratio of $F_{a,solid}$ to $F_{a,solution}$. The numerical value of $F_{a,solution}$ for lipophilic drugs is assumed to be 1 because the drugs are administered as a solution and complete absorption is possible due to their high permeability.

$$F_{a,solid} = rel.BA_{solid/solution} \quad (11)$$

MATERIALS AND METHODS

Materials

Danazol, griseofulvin, and cremophor EL were purchased from Sigma Chemical (St. Louis, MO, USA). Aprepitant was isolated from Emend® capsules (Merck & Co., Inc., Whitehouse Station, NJ, USA). Sodium taurocholate was purchased from Wako Pure Chemical Industries (Osaka, Japan). L-α-phosphatidylcholine was purchased from Nippon Oil and Fats Corporation (Tokyo, Japan). Vitamin ETPGS was purchased from Eastman Chemical Company (Kingsport, TN, USA). PEG400 was purchased from Dai-Ichi Kogyo Seiyaku Co., Ltd. (Kyoto, Japan).

The 0.45-μm polyvinylidene fluoride membrane filters (25 mm Automation Certified Filter Unit) for dissolution tests and the 0.4-μm polycarbonate filter plates (Multi-Screen® Solubility Plate) for the solubility studies were purchased from Millipore Corporation (Billerica, MA, USA).

The logD values and pKa values were calculated from the chemical structures of the drugs using Pallas 3.0 software (CompuDrug, Budapest, Hungary).

Preparation of Solid Particles of the Model Drugs for *In Vitro* and *In Vivo* Studies

Danazol crystals (melting point (mp) 224°C) and griseofulvin crystals (mp 219°C) were obtained by recrystallization in acetone and in a mixture of tetrahydrofuran and heptane, respectively, and dried by vacuum pump after filtration. Sieve fractions of 100–150 μm with a volume mean diameter (VMD) of 229 μm for danazol and a VMD of 118 μm for griseofulvin were obtained by sieve classification using standard sieves (Tokyo Screen Co., Ltd., Tokyo, Japan).

Table I. Properties of Drugs Used in This Study

Drug name	Ionization property[a]	MW	logD (6.5)[a]
Danazol	Neutral	337.5	4.0
Griseofulvin	Neutral	352.8	2.9
Aprepitant	Weak base (pKa=4.38)	534.4	5.3

[a] pKa and logD values were calculated using Pallas 3.0 software.

Micronization was achieved by fluid energy milling (one cycle at 600 MPa, Jetmill A-O JET, Seishin Enterprise Co., Ltd., Tokyo, Japan), resulting in a VMD of 5 μm for danazol and 7 μm for griseofulvin. No changes in the crystal form or crystallinity were observed from powder X-ray diffraction or the differential scanning calorimetry in the milling process. Before the *in vitro* and *in vivo* studies, one part drug was mixed with nine parts lactose as an excipient to improve the wettability of the drug.

Aprepitant crystals (mp 252°C) were obtained by recrystallization in methanol and drying by vacuum pump after filtration. A sieve fraction of 100–150 μm (VMD 26 μm) was obtained. Aprepitant crystals were milled in water by high-pressure homogenization under two different conditions using a high-pressure emulsifier (Nanomizer System YSNM-2000AR, Yoshida Kikai Co., Ltd., Aichi, Japan) and then lyophilized. The two milling conditions for the aprepitant crystals, ten cycles at 50 MPa and 100 cycles at 100 MPa, resulted in VMDs of 5 and 2 μm, respectively. No other crystal forms or crystallinity changes were observed from the milling process. Before the *in vitro* and *in vivo* studies, the aprepitant particles were suspended in 0.5% methylcellulose aqueous solution at 2 mg/ml.

Particle size analysis included microscopic examination (VH-8000, VH-Z450, KEYENCE, Osaka, Japan) and image analysis using software (Image-Pro Plus 5.1J, MediaCybernetics, MD, USA) to measure the Feret's diameter of more than 1,000 particles.

Miniscale Dissolution Tests

Dissolution tests were carried out by paddle method (50 rpm, 50 ml) using a VK7010 dissolution station and a VK8000 dissolution sampling station (Vankel Technologies, Inc., Cary, NC, USA) with a 100-ml glass vessel (42 mm diameter×105 mm, Takao Manufacturing Co., Ltd., Kyoto, Japan) as previously reported (6).

In order to investigate the effect of dissolution media on prediction, fasted-state simulated canine intestinal fluid (FaSSIF$_{dog}$) and phosphate buffer (PB) were used for the miniscale dissolution test and the solubility study. FaSSIF$_{dog}$ is a physiologically biorelevant medium containing 5 mM sodium taurocholate and 1.25 mM lecithin in 29 mM of phosphate buffer (pH 6.5) and PB is a conventional phosphate buffer (50 mM, pH 6.5) without bile salt and lecithin (18,19).

Saturated Solubility Study

The saturated solubility of the drugs was determined after 24 h of equilibration in media at 37°C using a shaking incubator. A 96-well polypropylene plate containing 0.5 ml of media per well was positioned in the incubator. Excess amounts of drugs were then added to the wells and experiments were carried out in triplicate. After 24 h, the aqueous samples were filtered through a 0.4-μm polycarbonate isopore membrane. The first 0.2 ml was discarded to avoid loss of drug from the sample due to adsorption. The remainder of the sample was diluted with an equal volume of tetrahydrofuran, including 0.8 mg/ml of *p*-hydroxybenzoic acid *n*-dodecyl ester as an internal standard.

High-Performance Liquid Chromatography Analysis of the Miniscale Dissolution Test and Saturated Solubility Study

Sample concentrations of both the dissolution test and the solubility study were determined by high-performance liquid chromatography (HPLC; Waters 2795 separation module, Waters, Milford, MA, USA) using a UV detector (Waters 2487 dual λ UV/VIS detector, Waters). Diluted samples (10 μl) were injected onto a C18 column (Cadenza CD-C18 3 μm 3.0×50 mm, Imtakt Corporation, Kyoto, Japan). Danazol, griseofulvin, and aprepitant were eluted with a mobile phase of water–acetonitrile–trifluoroacetic acid at ratios (by volume) of 55:45:0.1, 50:50:0.1 and 30:70:0.1, respectively, followed by the mobile ratio of 5:95:0.1 to elute *p*-hydroxybenzoic acid *n*-dodecyl ester as an internal standard, and were quantified with variable UV detection at 284, 320 and 230 nm, respectively. The detection wavelength for *p*-hydroxybenzoic acid *n*-dodecyl ester was 270 nm. A standard curve was prepared for each drug and linearity was observed at a concentration range of approximately 0.02–80 μg/ml on a log–log plot (correlation coefficient of r^2>0.999) by linear regression analysis using Microsoft Excel 2000 (Microsoft, Redmond, WA, USA).

In Vivo Oral Administration Study in Beagle Dogs

Danazol, griseofulvin, and aprepitant were administered orally to five Beagle dogs (male, body weight 12–15 kg). A washout period of 1 week was maintained between consecutive dosings. The dogs were fasted and water intake restricted overnight and for 8 h post-dosing. Following oral dosing, dogs were given 4 ml/kg of water.

All procedures using animals were conducted in accordance with the ethical guidelines for animal care promulgated by Chugai Pharmaceutical Co, Ltd., and all experimental protocols were approved by the Institutional Animal Care and Use Committee in Chugai.

Two sizes of danazol solid particles in capsules were each orally administered at a dose of 2 mg/kg. In order to investigate the dose effect on danazol absorption, smaller particles were also administered at a dose of 0.2 mg/kg. An aqueous danazol solution composed of 10% dimethyl sulfoxide (DMSO) and 20% vitamin ETPGS as solubilizers was orally administered at doses of 2 and 0.2 mg/kg. A danazol solution consisting of 5% EtOH, 25% dimethylacetamide, and 70% saline was intravenously administered at a dose of 0.0625 mg/kg. Two sizes of griseofulvin solid particles in capsules were each orally administered at a dose of 2 mg/kg. The smaller griseofulvin particles were also orally administered at a dose of 0.2 mg/kg. An aqueous griseofulvin solution in 10% DMSO and 90% PEG400 was orally administered at doses of 2 and 0.2 mg/kg. A griseofulvin solution consisting of

5% EtOH, 25% dimethylacetamide, and 70% saline was intravenously administered at a dose of 0.5 mg/kg. Three different sizes of aprepitant particles suspended in 0.5% methylcellulose solution and an aprepitant aqueous solution consisting of 10% DMSO and 5% cremophor EL as solubilizers were each orally administered at a dose of 2 mg/kg. Another aprepitant solution consisting of 5% EtOH, 25% dimethylacetamide, and 70% saline was intravenously administered at a dose of 0.0625 mg/kg. To maintain a high gastric pH, dogs were intravenously treated with famotidine (10 mg/dog) 2 h before the aprepitant administrations. Blood samples (1 ml) were collected from a foreleg vein with a heparinized syringe at 0 (pre-dose), 0.25, 0.5, 1, 2, 4, 8, 24, and 48 h after oral administration and 0 (pre-dose), 0.08, 0.25, 0.5, 1, 2, 4, 8, 24, and 48 h after intravenous administration. Plasma samples were obtained by centrifugation of the blood samples and stored at −20°C until use.

Analysis of Plasma Concentration

Plasma concentration was quantified by HPLC mass spectroscopy (LC–MS/MS). Dog plasma was spiked with danazol in MeOH to yield concentrations for a standard curve. To 100 μl of plasma standard and unknowns, 10 μl of 50% MeOH aqueous solution, 100 μl of water, and 20 μl of MeOH including 0.1 μmol/l of methyltestosterone as an internal standard (IS) were added. The samples were extracted using a solid phase extraction kit (Oasis μElution Plate® HLB, SPE cartridges, Waters). The concentration of danazol in plasma was determined by LC–MS/MS using a Shimadzu 10A Separations Module (Shimadzu, Kyoto, Japan) connected to an API4000™ LC–MS/MS system (Applied Biosystems, Foster City, CA, USA) with a C18 column (Capcell Pack C18 UG120 5 μm 2.0×250 mm, Shiseido, Tokyo, Japan). The eluents consisted of water–acetonitrile at a ratio of 10:90 delivered at 0.2 ml/min. The injection volume was 25 μl. The MS/MS instrument was operated in atmospheric pressure chemical ionisation (APCI). Detection was performed in the positive-ion mode using selected reaction monitoring (SRM) of the *m*/*z* 338–115 and *m*/*z* 303–109 transitions for danazol and the IS, respectively; collusion energies of 95 and 37 eV were used for danazol and the IS, respectively. The $(1/\chi^2)$ linear regression analysis showed correlation coefficients of linearity (r^2>0.999) at concentration ranges of 0.3–1,000 ng/ml.

Dog plasma was spiked with griseofulvin or aprepitant in EtOH to yield concentrations for a standard curve. For griseofulvin, 10 μl of 50% MeOH aqueous solution, 100 μl of water, and 20 μl of MeOH including 0.1 μmol/l of warfarin as an IS were added to 50 μl of plasma standard and unknowns. For aprepitant, 10 μl of 50% MeOH aqueous solution, 100 μl of water, and 20 μl of MeOH including 0.1 μmol/l of danazol as an IS were added to 5 μl of plasma standard and unknowns. The samples were extracted using the Oasis μElution solid phase extraction kit previously mentioned. The concentration of griseofulvin and aprepitant in plasma was determined by LC–MS/MS using a Shimadzu 10A Separations Module connected to a Q TRAP® LC-MS/MS system (Applied Biosystems) with a C18 column (Unison UK-C8 30 mm×2 mm, Imtakt Corporation). The eluents consisted of water–acetonitrile–formic acid at a ratio of 95:5:0.1 (solvent A) and 5:95:0.1 (solvent B). Elution was accomplished using a linear gradient that consisted of ramping solvent B from 0% to 100% over 1.7 min at a flow rate of 0.4 ml/min. The injection volume was 10 μl. The MS/MS instrument was operated in electrospray ionisation mode. Detection was performed in the positive-ion mode using SRM of *m*/*z* 353–165 and *m*/*z* 309–251 transitions for griseofulvin and the IS, *m*/*z* 535–277 and *m*/*z* 338–310 transitions for aprepitant and the IS, respectively; collusion energy of 30 eV was used for griseofulvin, aprepitant and there is for each.

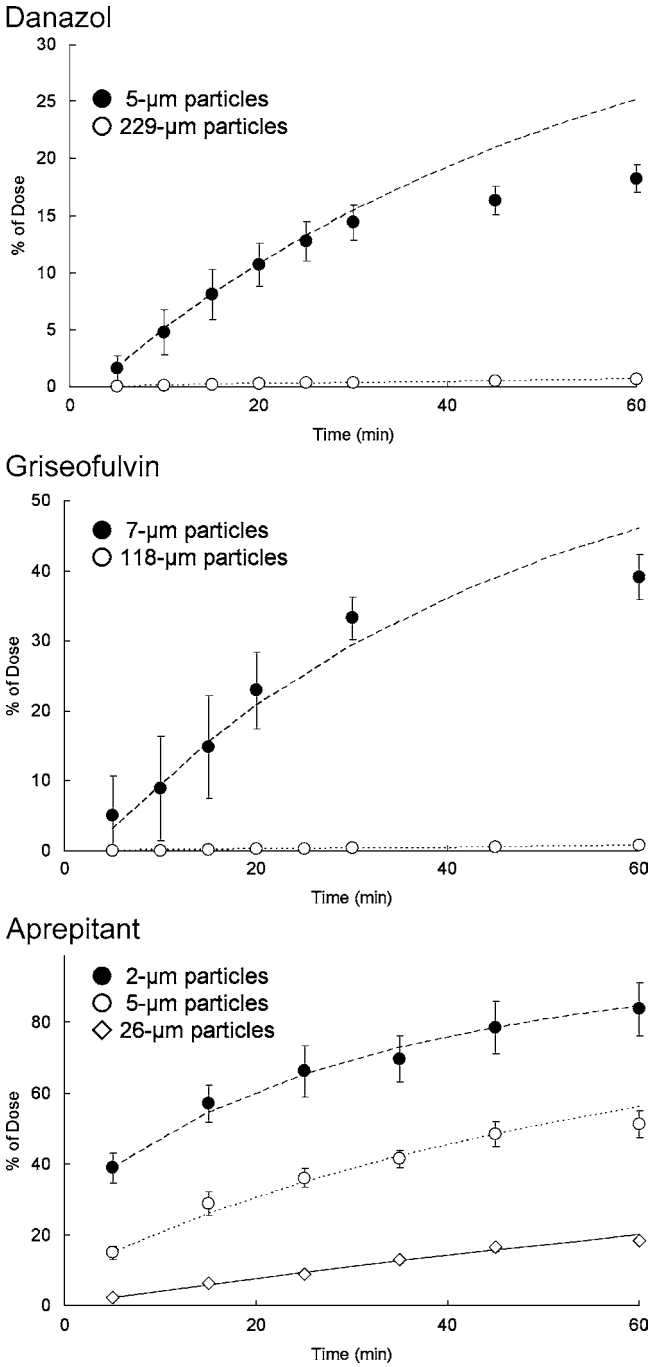

Fig. 1. Time profiles of the cumulative percentage dissolved and fitting curves (*dotted and solid lines*) for several different particle sizes of *danazol*, *griseofulvin*, and *aprepitant* in $FaSSIF_{dog}$. Fitting curves were obtained assuming that the drugs dissolved according to the Noyes–Whitney equation.

The equivalency of ion suppression between griseofulvin and the IS and aprepitant and the IS was determined by QC analysis of individual dog plasma. The ($1/\chi^2$) linear regression analysis showed correlation coefficients of linearity ($r^2 > 0.993$) within a concentration range of 4–512 ng/ml for griseofulvin and 1–1,024 ng/ml for aprepitant.

PK Analysis

The pharmacokinetic parameters were determined using noncompartmental analysis (WinNonlin, version 4.0.1, Pharsight Corporation, Mountain View, CA, USA). The AUC was calculated from 0 to infinity using a linear trapezoidal rule. The *in vivo* absorption–time profiles of drugs were estimated using a numerical deconvolution technique. The mean plasma concentration data from the oral administration study was designated the response function, and data from the intravenous administration study was designated the weight function. After calculating the BA–time profiles of all oral administrations, the BA value at each time point for solid particles was divided by that of the solution administration at 48 h to obtain F_a time profiles of the solid administrations. The BA values for solution administrations of danazol and griseofulvin were constant throughout doses of 0.2 to 2 mg/kg, indicating systemic pharmacokinetics linearity for this range of plasma concentration.

$$F_{a,solid,t} = \frac{BA_{solid,t}}{BA_{solution,48h}} \times 100 \quad (12)$$

$F_{a,solid,t}$ is the fraction absorbed at time t. $BA_{solid,t}$ and $BA_{solution,48\ h}$ are respectively the bioavailability of the solid administration at time t and the solution administration at 48 h determined by deconvolution analysis.

Permeation Experiments in Caco-2 Monolayers

In order to ensure high permeability of the model drugs, permeation experiments in Caco-2 monolayers were performed as described previously (6).

RESULTS

Miniscale Dissolution Test, Solubility Study, and Unstirred Water Layer Permeability Calculations

The dissolution profiles of danazol, griseofulvin, and aprepitant in the miniscale dissolution test with $FaSSIF_{dog}$ were illustrated in Fig. 1. The dissolution parameters (z) of these three drugs in $FaSSIF_{dog}$ and PB were extracted for each particle size from the fitting curve in Fig. 1 and summarized in Table II. z values were inversely proportional to the particle size for all drugs. The saturated solubility of danazol, griseofulvin, and aprepitant was determined to be 7, 16, and 21 μg/ml in $FaSSIF_{dog}$ and 0.7, 14, and 0.8 μg/ml in PB, respectively. UWL permeability is shown in Table II.

In Vivo Oral Administration Study

The *in vivo* oral administration study with the different-sized danazol particles (Fig. 2, Table III) showed that the AUC value of plasma concentration after the administration of smaller particles (VMD: 5 μm) was six times greater than that of the larger particles (229 μm). The griseofulvin AUC from the smaller particles (7 μm) was 16 times greater than from the larger ones (118 μm). The aprepitant AUC after administration of 2-μm particles was 1.2 and 1.8-fold larger than that of 5- and 26-μm particles, respectively, and considered not statistically significant. These results indicate that the effect of particle size on oral absorption varies among drugs. However, the plasma concentrations from solutions of the three drugs were much higher than those from even the smallest particles, indicating a limit of absorption from solid dosage forms. In Table III, a comparison of the AUC values for the two doses (2 and 0.2 mg/kg) of the smaller particles of danazol and griseofulvin were respectively only five and six times greater, not tenfold, thus exhibiting saturated and dose nonlinear absorption.

Permeability Measurement and Calculation

The P_{app} values of the three drugs were measured in Caco-2 monolayers. The P_{app} of danazol, griseofulvin, and aprepitant was 8.7±5.0, 4.5±1.0, and 2.1±0.9 10^{-5} cm/s, respectively. The contribution of the UWL to drug permeation through the Caco-2 membrane was different from that through *in vivo* intestinal membrane because the experimental conditions such as agitation speed were not the same as *in vivo*. Also, the surface of the intestinal membrane, but not of Caco-2 monolayers, are covered with mucus layer which may form the thicker UWL. We previously reported that the UWL on the membrane was the main source of the resistance to permeation across the intestinal membrane for lipophilic drugs (0.7–6.5 of logD (6.5), 2.7–10.1×10^{-5} cm/s of Caco-2 permeability) (6). In that report, the calculated P_{UWL} of ketoprofen (9×10^{-4} cm/s) was nearly equal to reported

Table II. Dissolution Parameter z Obtained From the Dissolution Curve, the Saturated Solubility of Three Compounds in $FaSSIF_{dog}$, and PB (Mean±SD) and the Calculated Unstirred Water Layer Permeability Used for the Simulation

Drug name	Mean particle diameter (μm)	z (ml mg^{-1} min^{-1})		C_s (mg ml^{-1})		P_{UWL} 10^{-3} (cm s^{-1})
		$FaSSIF_{dog}$	PB	$FaSSIF_{dog}$	PB	
Danazol	5	0.912±0.159	1.973±0.433	0.007±0.000	0.0007±0.0000	1.3
	229	0.014±0.004	0.063±0.027			
Griseofulvin	7	1.005±0.206	1.442±0.092	0.016±0.000	0.014±0.0000	1.3
	118	0.008±0.002	0.008±0.001			
Aprepitant	2	1.900±0.591	3.366±1.251	0.021±0.004	0.0008±0.0001	1.1
	5	0.756±0.093	2.171±0.403			
	26	0.183±0.013	0.135±0.034			

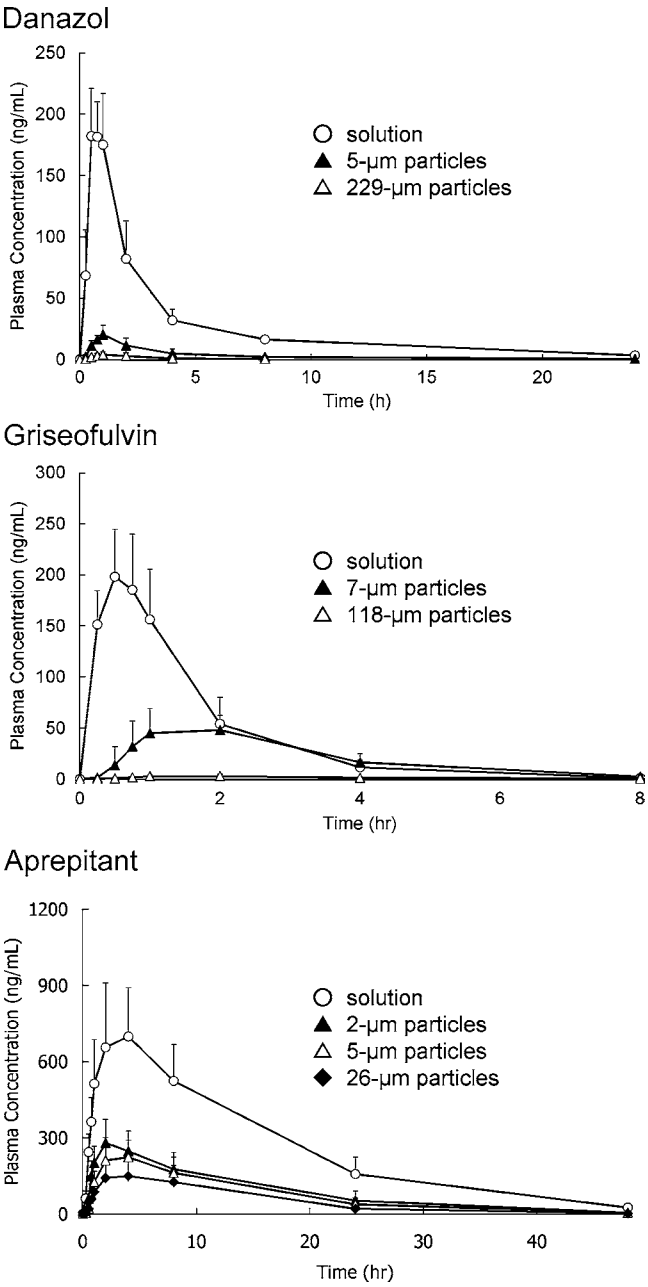

Fig. 2. Mean (±SD) plasma concentrations of *danazol*, *griseofulvin*, and *aprepitant* following oral administration in Beagle dogs (n=5) under fasted conditions at a dose of 2 mg/kg. Dogs were intravenously treated with famotidine to maintain high gastric pH before administration of aprepitant.

human jejunal permeability (9×10^{-4} cm/s) despite the fact that the P_{UWL} of ketoprofen was much greater than Caco-2 P_{app} (6×10^{-5} cm/s). In this study, therefore, considering their high Caco-2 membrane permeability and high lipophilicity, it is reasonable to assume that permeation of the model drugs through the intestinal wall was limited by diffusion through the UWL.

Oral Absorption Prediction

In order to predict the oral absorption and rate limiting steps of different-sized particles of the model drugs, the amount of solid drug, $X_{s,vivo}(t)$, and dissolved drug, $X_{d,vivo}(t)$, in the intestinal tract and absorbed drug, $X_{a,vivo}(t)$, was simulated from Eqs. 5–8 using the saturated solubility and z values obtained from the miniscale dissolution test, UWL permeability, and oral administration in dogs (Table II).

In Fig. 3, the time-profiles of F_a were obtained from the *in vivo* oral administration study in dogs. The data of intravenous administration were used for numerical deconvolution analysis. Fig. 3 also shows the simulation of time-profiles of F_a from *in vitro* dissolution and solubility data for $FaSSIF_{dog}$. For all drugs, simulated F_a well reflected the data observed *in vivo* showing dissolution rate-dependent absorption. The predicted F_a of each drug, calculated from the amount of simulated absorption after 2 h and the administered dose, correlated well with observed F_a (Table III). In contrast, when PB was used as the media for the *in vitro* dissolution test, the simulated F_a was much less than the observed results for danazol and aprepitant (Fig. 3). However, in the case of griseofulvin, PB gave almost the same results as $FaSSIF_{dog}$.

To investigate the rate limiting steps of oral absorption for each different-sized and different-dosed solid particle, the intestinal drug concentration ($X_{d,vivo}(t)/V$) was simulated and given as a ratio of the drug saturated solubility, $C(t)_{ratio}$. The time–intestinal drug concentration profiles simulated from the *in vitro* dissolution test with $FaSSIF_{dog}$ are shown in Fig. 4. The $C(t)_{ratio}$ after administration of the two sizes of danazol particles (VMD 5 and 229 μm) was simulated to be about 85% and 8%, respectively, at a dose of 2 mg/kg and about 30% at a dose of 0.2 mg/kg (5 μm). The $C(t)_{ratio}$ of the two sizes of griseofulvin particles (7 and 118 μm) was also simulated to be 85% and 5%, respectively, and 18–34% at a dose of 0.2 mg/kg (5 μm). For aprepitant, the $C(t)_{ratio}$ for each particle size (2, 5, and 26 μm) was simulated to be 92%, 83%, and 55%, respectively, at a dose of 2 mg/kg. If the ratio of the intestinal drug concentration at time t against the drug saturated solubility, $C_{ratio}(t)$, is low (sink conditions), drug absorption is considered to be limited by the dissolution rate (Fig. 4). On the other hand, if $C_{ratio}(t)$ increases and approaches unity, absorption is limited not only by the dissolution rate but also by saturated solubility. Our simulation showed that the concentration of danazol and griseofulvin in the intestine after the administration of large particles remained quite low compared to the saturated solubility, suggesting that absorption was limited by the dissolution rate. In the case of the smaller particles, it was predicted that drug concentration in the intestine would became high, indicating that absorption was limited not by the dissolution rate but by solubility.

DISCUSSION

Insufficient exposure of poorly water-soluble drugs such as BCS class II (20) from oral administration due to a lack of or nonlinear drug absorption often makes it difficult to evaluate drug efficacy and safety in both the preclinical and the clinical stage of development. The model drugs used in this study were classified as BCS class II because the dose number is more than 1 and permeability through the Caco-2 monolayer is higher than metoprolol (0.5×10^{-5} cm/s, in-house data). In order to quantitatively predict oral absorption of BCS class II drugs, we simulated drug concentration in the

Table III. Pharmacokinetic Parameters and Observed F_a in Dogs (Mean±SD, n=5), and Predicted F_a for Danazol, Griseofulvin, and Aprepitant

Drug name	Particle size (admin form)	Dose (mg kg^{-1})	AUC (ng h ml^{-1})	BA[a] (%)	Observed F_a[b] (%)	Predicted F_a[c] (%)	
						$FaSSIF_{dog}$	PB
Danazol	Solution	2	613.8±135.9	13.8±3.8	100	–	–
	5 μm (solid)	2	74.1±30.0	1.7±0.7	12.1±5.6	11	1
	229 μm (solid)	2	12.1±6.1	0.3±0.1	2±1.1	1	0.4
	Solution	0.2	47.6±10.3	10.7±2.9	100	–	–
	5 μm (solid)	0.2	14.2±2.8	3.2±0.8	29.8±8.7	41	7
Griseofulvin	Solution	2	331.3±121.0	25.9±12.6	100	–	–
	7 μm (solid)	2	155.2±47.5	12.2±5.4	46.9±22.3	25	23
	118 μm (solid)	2	9.5±4.6	0.7±0.4	2.9±1.7	1	1
	Solution	0.2	31.4±8.0	24.6±10	100	–	–
	7 μm (solid)	0.2	26.6±4.3	20.8±7.4	84.9±24.4	80	84
Aprepitant[d]	Solution	2	11,478.4±3,497.5	83.4±26.2	100	–	–
	2 μm (suspn)	2	3,814.2±1,621.1	27.7±12	33.2±17.4	32	1
	5 μm (suspn)	2	3,179.0±1,428.7	23.1±10.5	27.7±15	28	1
	26 μm (suspn)	2	2,091.8±1,094.3	15.2±8	18.2±11	18	0.6

[a] BA was calculated from the dose-normalized AUCs (AUC/dose) after intravenous and oral administrations.
[b] Observed F_a was calculated from AUCs of solid and solution dosage forms.
[c] Predicted F_a using the dissolution results in $FaSSIF_{dog}$ and PB.
[d] Dogs were intravenously treated famotidine 2 h before aprepitant administration to maintain high gastric pH.

intestinal tracts (Fig. 4), which is essential for recognizing the rate-limiting steps of oral absorption. For the larger solid particles of danazol, griseofulvin, and aprepitant, dissolution in the small intestine was simulated to occur under a sink condition in which oral absorption is certainly dissolution-rate-limited. Particle size reduction had a significant impact on the dissolution rate *in vitro*, on the simulated oral absorption, and on the absorption observed in dogs. The dissolution of the smaller particles of danazol, griseofulvin, and aprepitant in the small intestine occurred under a nonsink condition in the simulation, indicating solubility-limited absorption. In fact, dose nonlinearity was observed with the smaller particles of danazol and griseofulvin in dogs. For aprepitant, particle size reduction to 2-μm did not significantly improve oral absorption *in vivo* even though the dissolution rate increased. Increasing the dissolution rate of smaller particles of the model drugs would no longer improve their oral absorption despite lower plasma concentrations than the solution administration because oral absorption of the small particles is limited by solubility and not by dissolution rate.

A clear understanding of the rate-limiting process of oral absorption is crucial for improving oral absorption. Our results suggest that the rate-limiting steps on oral absorption shift from dissolution rate-limited to solubility-limited even for the same drug as they do with an increase in either the dissolution rate or the administration dose. Oral absorption *in vivo* of danazol was clearly improved by particle size reduction, suggesting that absorption of danazol from larger particles was limited by the dissolution rate; however, oral absorption of the smaller particles *in vivo* resulted in an 11-fold increase, indicating a non-proportional change when compared to the 65-fold increase in the dissolution rate observed with the larger particles. In addition, the absorption of danazol did not show linear correlation with dose (0.2–2 mg/kg), indicating that absorption from small particles at 2 mg/kg was limited not by the dissolution rate but by solubility. Similar results were also observed with griseofulvin. The fraction of dose absorbed of danazol and griseofulvin after administration of different-sized particles showed nonlinearity with the dissolution rate (Fig. 5, griseofulvin data not shown). In addition, when the smaller particles were administered, the absorbed amount was simulated to peak at a high dose (Fig. 6) because the dissolution from small particles occurred under nonsink conditions at the dose of 2 mg/kg. For aprepitant, improvement of oral absorption from particle size reduction of the 5- to 2-μm particles was less than for the 26-μm particles. The simulated $C_{ratio}(t)$ for the 26-μm particles was approximately 50%, which means that oral absorption remained dissolution-rate-limited. Thus, particle size reduction improved oral absorption for the 26-μm particles of aprepitant. But for the 5-μm particles, further size reduction was less effective because the rate-limiting step of oral absorption shifted to solubility. In order to improve solubility-limited absorption such as absorption from smaller particles of danazol, griseofulvin and aprepitant, increased solubility is most likely required. Some solid forms such as salts, cocrystals and amorphous forms often exhibit higher drug solubility (21). Moreover, several formulation technologies that allow super-saturation such as solid dispersion and lipid formulation are useful for improving drug solubility in the small intestine (22,23). Our results, in which simulated F_a correlated well with observed F_a, indicate that our method of simulating drug dissolution and permeation processes in the intestinal tract reflects *in vivo* drug dissolution both under sink and nonsink conditions and helps clarify the rate-limiting steps of drug absorption. Our system can be used to determine an appropriate strategy to improve both dissolution rate-limited and solubility-limited absorption of a drug dissolved in the intestine but not in the stomach and colon.

The *in vitro* dissolution profile in a biorelevant medium showed better estimations of oral absorption than the conventional buffer without bile and lecithin. The saturated solubility of the model drugs was higher in $FaSSIF_{dog}$ than in

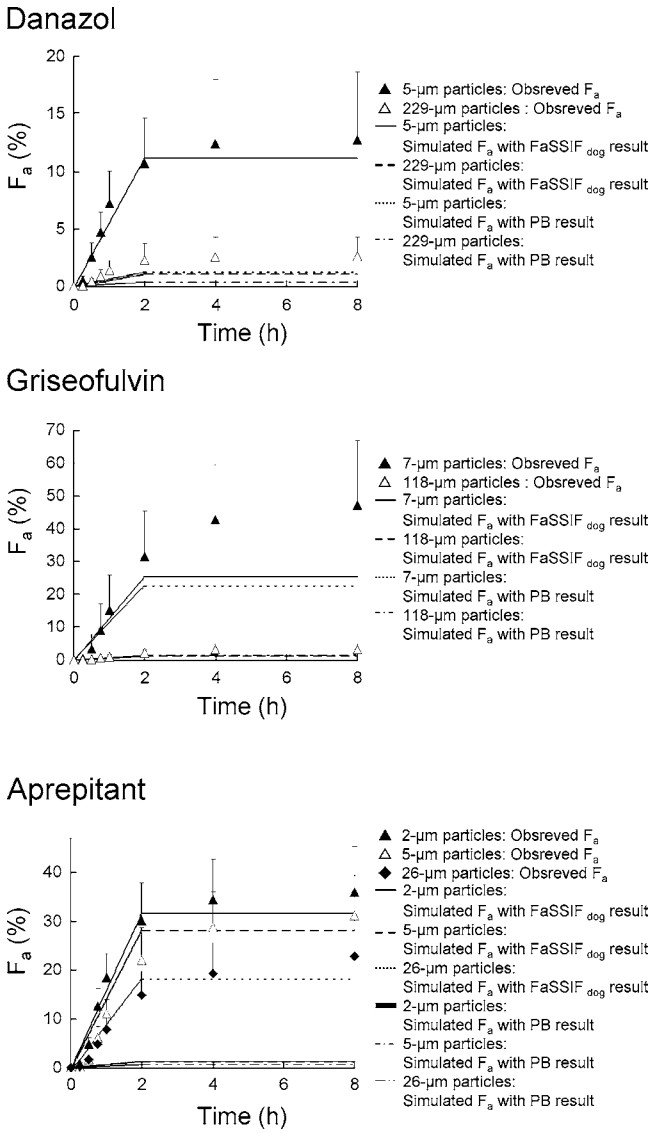

Fig. 3. Comparison of the observed and simulated F_a time profiles of *danazol*, *griseofulvin*, and *aprepitant*. Observed F_a was determined using a numerical deconvolution technique following oral administration in Beagle dogs (n=5) under fasted conditions at a dose of 2 mg/kg. The deconvolution analysis was carried out using the plasma concentration data from the oral administration study as the response function and the data from the intravenous administration study as the weight function. The relative bioavailability of a solid dosage form and a solution orally administered served as the F_a. Results are expressed as the mean; bars indicate SD value. Predicted F_a was simulated by solving Eqs. 5–8 with the dissolution results both in $FaSSIF_{dog}$ and in PB.

PB due to the solubilizing effect of the micelles in $FaSSIF_{dog}$ (24–26). When the PB results were used, simulated oral absorption was lower than observed absorption and the effect of particle size was unclear. These results indicate that physiologically biorelevant media are important for the investigation of oral absorption and the rate-limiting steps of poorly water-soluble drugs.

The miniscale dissolution test clearly detected the change in the drug dissolution rate caused by particle size reduction. The dissolution rate of small particles of danazol was 65-times faster than that of large particles in $FaSSIF_{dog}$. The two smaller-sized particles of aprepitant showed four and ten times faster dissolution than the larger particles and had good correspondence with particle size reduction (46-, 5-, and 11-fold, respectively), suggesting that the dissolution of danazol and aprepitant can be determined by the Noyes–Whitney

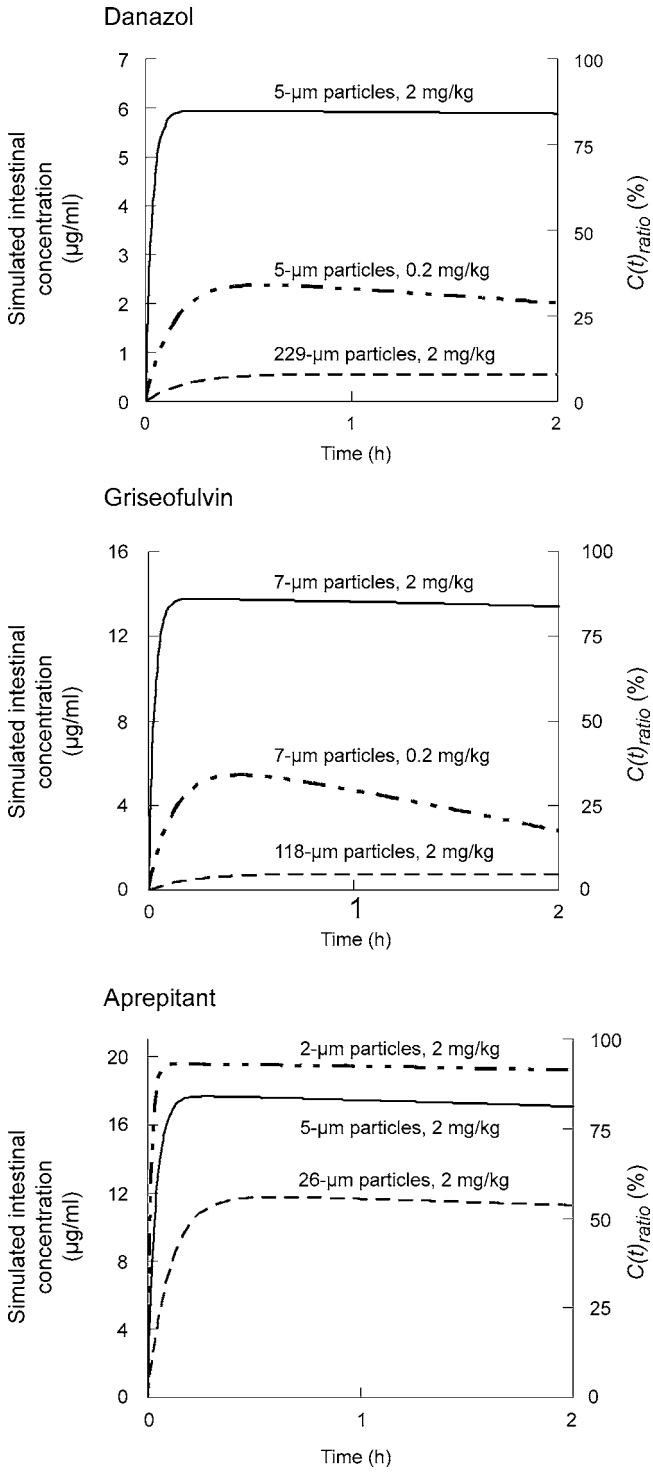

Fig. 4. Simulated intestinal drug concentration, $X_{d,vivo}(t)/V_{vivo}$, and the percentage of the intestinal drug concentration against the saturated solubility, $C_{ratio}(t)$, from different-sized particles of *danazol*, *griseofulvin* and *aprepitant* using Eqs. 5–9 with the dissolution results in $FaSSIF_{dog}$.

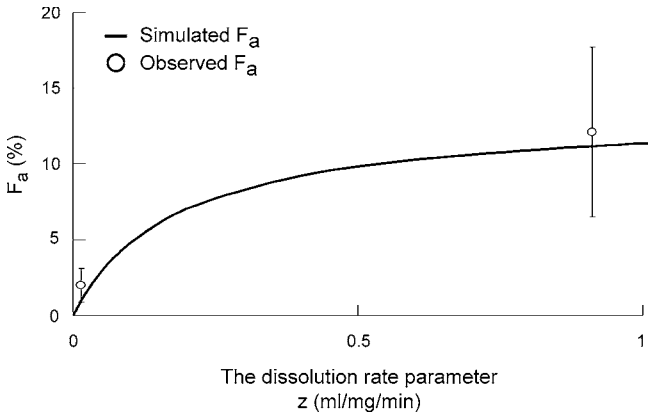

Fig. 5. Simulated F_a of danazol in dogs as a function of the dissolution rate parameter z at a dose of 2 mg/kg (*line*) and observed F_a from small (z=0.912) and large (z=0.014) particles (*circle*, mean±SD).

theory. In contrast, the dissolution of small-particle griseofulvin was 125 times faster than that of the larger particle, even though the particles were only ten times smaller. The disagreement in the ratio of dissolution rate and particle size with griseofulvin might be because of the lozenge-shaped particles, making it difficult to clearly represent the surface area. It is important to determine the dissolution rate experimentally when quantitatively predicting the oral absorption of a drug.

The predicted F_a of griseofulvin at a dose of 2 mg/kg was half of the mean observed value. The reason for this disagreement is unclear but might be related to the absorption site of griseofulvin in the GI tract. Although an intestinal transit time of 2 h limited the absorption time in our prediction, the real absorption time *in vivo* of griseofulvin appeared to be longer than 2 h (Fig. 3). According to the time profiles of *in vivo* absorption, 30% of the griseofulvin was absorbed within 2 h and our simulation also showed 30% absorption of griseofulvin within 2 h (Fig. 3), indicating a quantitative prediction of the absorption rate. Griseofulvin absorption *in vivo* continued for 8 h and had increased by almost twofold the amount absorbed within 2 h, suggesting that griseofulvin is possibly absorbed not only in the small intestine but also in the colon (27). Understanding how the solubility and permeability characteristics of griseofulvin, the transit time, and the hydrodynamics in the colon are different from those in the small intestine would be necessary to take the absorption from the colon into account.

There is some discrepancy between the experimental and fitted dissolution lines at the latter part of the dissolution for danazol and griseofulvin despite the successful fitting at the beginning and the middle (Fig. 1). This may be a result of the particle size distribution in the drug. With particles of different sizes, small particles are possibly completely dissolved and diminished earlier than large ones. Therefore, a greater number of large particles in the distribution would have more of an effect on the dissolution rate at the latter part of the dissolution. Our model may not reflect the effect of larger particles in the dissolution because we assume the drug to be a monodispersed powder. Hints *et al*. reported that the amount of small and large particles in the distribution affect drug dissolution (28,29). The effect of particle size distribution on dissolution may explain these mismatches.

In the present study, data of absorption in dog rather than in human were used to validate our method of predicting the rate-limiting steps of oral absorption because suitable clinical data and formulations in human are not readily available. So it is necessary to consider interspecies differences to predict the rate-limiting steps of oral absorption in humans from data in dogs. The results from different dissolution media ($FaSSIF_{dog}$ and PB) clearly show that solubilization with bile salts is important in the oral absorption of poorly soluble drugs. It is known that there are differences in the composition of intestinal fluid in dogs and humans, including the concentration of bile salts (16,19). In order to simulate drug dissolution in the human intestine, biorelevant dissolution media with lower concentrations of bile salts and lecithin than in dogs should be used (30). Concerning membrane permeability, it has been reported that water-soluble neutral drugs are absorbed faster in dogs than in humans because the size of the tight junction for the paracellular transport pathway is greater in dogs than in humans (31). However, the permeability of highly permeable drugs in the intestine will not differ significantly between dog and human because the UWL diffusion rates are similar (10,15). The intestinal transit time in human is twice as long as in dog (16). Although the intestinal surface area and water volume are also species specific (17), the rate-limiting steps of human oral absorption could be identified by using human physiological parameters for the simulation.

In conclusion, elucidating the rate-limiting process of oral absorption helps us to better understand the cause of poor absorption of poorly water-soluble drugs. Our method requires only a small scale *in vitro* study to predict dose- and particle size-dependent absorption and therefore, can contribute to early stage studies in the pharmaceutical industry for the development of improved oral drug products.

ACKNOWLEDGMENTS

We would like to express our gratitude to Mr. Tessai Yamamoto for his helpful contribution to the plasma concentration analysis, Dr. Motohiro Kato for his help in the deconvolution analysis, Ms Atsuko Higashida for her help in the Caco-2 experiments, the pharmaceutical profiling group members for their help with the *in vivo* experiments, and Mr. Shoichi Higo for his helpful comments and suggestions.

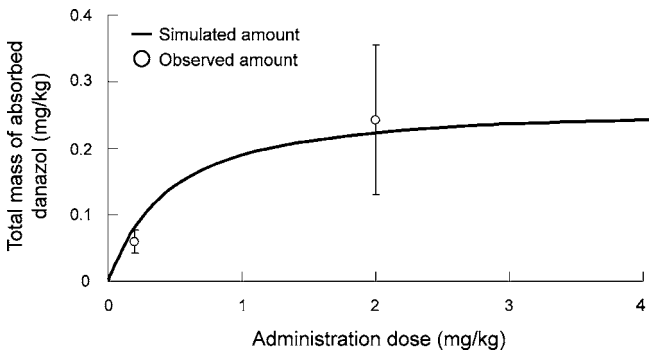

Fig. 6. Simulated absorbed amount of danazol ($X_{a,vivo}$(2 h)) from small particles (z=0.912) as a function of the administration dose (*line*) and the observed absorbed amount in dogs at doses of 0.2 and 2 mg/kg (*circle*, mean±SD).

REFERENCES

1. C. A. Lipinski. Drug-like properties and the causes of poor solubility and poor permeability. *J. Pharmacol. Toxicol. Methods.* **44**:235–249 (2000). DOI 10.1016/S1056-8719(00)00107-6.
2. L. X. Yu. An integrated model for determining causes of poor oral drug absorption. *Pharm. Res.* **16**:1883–1887 (1999). DOI 10.1023/A:1018911728161.
3. K. Sugano, A. Okazaki, S. Sugimoto, S. Tavornvipas, A. Omura, and T. Mano. Solubility and dissolution profile assessment in drug discovery. *Drug Metab. Pharmacokinet.* **22**:225–254 (2007). DOI 10.2133/dmpk.22.225.
4. B. Agoram, W. S. Woltosz, and M. B. Bolger. Predicting the impact of physiological and biochemical processes on oral drug bioavailability. *Adv. Drug Deliv. Rev.* **50**(Suppl 1):S41–S67 (2001). DOI 10.1016/S0169-409X(01)00179-X.
5. G. M. Grass, and P. J. Sinko. Physiologically-based pharmacokinetic simulation modelling. *Adv. Drug Deliv. Rev.* **54**:433–451 (2002). DOI 10.1016/S0169-409X(02)00013-3.
6. R. Takano, K. Sugano, A. Higashida, Y. Hayashi, M. Machida, Y. Aso, and S. Yamashita. Oral absorption of poorly water-soluble drugs: computer simulation of fraction absorbed in humans from a miniscale dissolution test. *Pharm. Res.* **23**:1144–1156 (2006). DOI 10.1007/s11095-006-0162-4.
7. A. A. Noyes, and W. R. Whitney. The rate of solution of solid substances in their own solutions. *J. Am. Chem. Soc.* **19**:930–934 (1987). DOI 10.1021/ja02086a003.
8. W. L. Hayton. Rate-limiting barriers to intestinal drug absorption: a review. *J. Pharmacokinet. Biopharm.* **8**:321–334 (1980). DOI 10.1007/BF01059381.
9. J. H. Kou, D. Fleisher, and G. L. Amidon. Calculation of the aqueous diffusion layer resistance for absorption in a tube: application to intestinal membrane permeability determination. *Pharm. Res.* **8**:298–305 (1991). DOI 10.1023/A:1015829128646.
10. H. Lennernas. Human intestinal permeability. *J. Pharm. Sci.* **87**:403–410 (1998). DOI 10.1021/js970332a.
11. M. D. Levitt, T. Aufderheide, C. A. Fetzer, J. H. Bond, and D. G. Levitt. Use of carbon monoxide to measure luminal stirring in the rat gut. *J. Clin. Invest.* **74**:2056–2064 (1984). DOI 10.1172/JCI111629.
12. D. Winne, H. Gorig, and U. Muller. Closed rat jejunal segment *in situ*: role of pre-epithelial diffusion resistance (unstirred layer) in the absorption process and model analysis. *Naunyn. Schmiedebergs Arch. Pharmacol.* **335**:204–215 (1987). DOI 10.1007/BF00177725.
13. D. Winne. Unstirred layer thickness in perfused rat jejunum *in vivo*. *Experientia.* **32**:1278–1279 (1976). DOI 10.1007/BF01953092.
14. K. Obata, K. Sugano, R. Saitoh, A. Higashida, Y. Nabuchi, M. Machida, and Y. Aso. Prediction of oral drug absorption in humans by theoretical passive absorption model. *Int. J. Pharm.* **293**:183–192 (2005). DOI 10.1016/j.ijpharm.2005.01.005.
15. M. D. Levitt, J. K. Furne, A. Strocchi, B. W. Anderson, and D. G. Levitt. Physiological measurements of luminal stirring in the dog and human small bowel. *J Clin. Invest.* **86**:1540–1547 (1990). DOI 10.1172/JCI114873.
16. J. B. Dressman. Comparison of canine and human gastrointestinal physiology. *Pharm. Res.* **3**:123–131 (1986). DOI 10.1023/A:1016353705970.
17. T. T. Kararli. Comparison of the gastrointestinal anatomy, physiology, and biochemistry of humans and commonly used laboratory animals. *Biopharm. Drug Dispos.* **16**:351–380 (1995). DOI 10.1002/bdd.2510160502.
18. A. Scholz, E. Kostewicz, B. Abrahamsson, and J. B. Dressman. Can the USP paddle method be used to represent *in-vivo* hydrodynamics? *J. Pharm. Pharmacol.* **55**:443–451 (2003). DOI 10.1211/002235702946.
19. L. Kalantzi, E. Persson, B. Polentarutti, B. Abrahamsson, K. Goumas, J. B. Dressman, and C. Reppas. Canine intestinal contents *vs*. simulated media for the assessment of solubility of two weak bases in the human small intestinal contents. *Pharm. Res.* **23**:1373–1381 (2006). DOI 10.1007/s11095-006-0207-8.
20. N. A. Kasim, M. Whitehouse, C. Ramachandran, M. Bermejo, H. Lennernas, A. S. Hussain, H. E. Junginger, S. A. Stavchansky, K. K. Midha, V. P. Shah, and G. L. Amidon. Molecular properties of WHO essential drugs and provisional biopharmaceutical classification. *Mol. Pharm.* **1**:85–96 (2004). DOI 10.1021/mp034006h.
21. S. L. Morissette, O. Almarsson, M. L. Peterson, J. F. Remenar, M. J. Read, A. V. Lemmo, S. Ellis, M. J. Cima, and C. R. Gardner. High-throughput crystallization: polymorphs, salts, co-crystals and solvates of pharmaceutical solids. *Adv. Drug Deliv. Rev.* **56**:275–300 (2004). DOI 10.1016/j.addr.2003.10.020.
22. P. C. Porter, J. F. Cuine, and W. N. Charman. Enhancing intestinal drug solubilisation using lipid-based delivery systems. *Adv. Drug Deliv. Rev.* **60**:673–691 (2008).
23. R. J. Chokshi, H. Zia, H. K. Sandhu, N. H. Shah, and W. A. Malick. Improving the dissolution rate of poorly water soluble drug by solid dispersion and solid solution: pros and cons. *Drug Deliv.* **14**:33–45 (2007). DOI 10.1080/10717540600640278.
24. V. J. Stella, S. Martodihardjo, and V. M. Rao. Aqueous solubility and dissolution rate does not adequately predict *in vivo* performance: a probe utilizing some *N*-acyloxymethyl phenytoin prodrugs. *J. Pharm. Sci.* **88**:775–779 (1999). DOI 10.1021/js980489i.
25. E. Nicolaides, M. Symillides, J. B. Dressman, and C. Reppas. Biorelevant dissolution testing to predict the plasma profile of lipophilic drugs after oral administration. *Pharm. Res.* **18**:380–388 (2001). DOI 10.1023/A:1011071401306.
26. M. Kataoka, Y. Masaoka, Y. Yamazaki, T. Sakane, H. Sezaki, and S. Yamashita. *In vitro* system to evaluate oral absorption of poorly water-soluble drugs: simultaneous analysis on dissolution and permeation of drugs. *Pharm. Res.* **20**:1674–1680 (2003). DOI 10.1023/A:1026107906191.
27. A. L. Ungell, S. Nylander, S. Bergstrand, A. Sjoberg, and H. Lennernas. Membrane transport of drugs in different regions of the intestinal tract of the rat. *J. Pharm. Sci.* **87**:360–366 (1998). DOI 10.1021/js970218s.
28. R. J. Hintz, and K. C. Johnson. The effect of particle size distribution on dissolution rate and oral absorption. *Int. J. Pharm.* **51**:9–17 (1989). DOI 10.1016/0378-5173(89)90069-0.
29. A. Okazaki, T. Mano, and K. Sugano. Theoretical dissolution model of poly-disperse drug particles in biorelevant media. *J. Pharm. Sci.* **97**:1843–1852 (2007). DOI 10.1002/jps.21070.
30. E. Galia, E. Nicolaides, D. Horter, R. Lobenberg, C. Reppas, and J. B. Dressman. Evaluation of various dissolution media for predicting *in vivo* performance of class I and II drugs. *Pharm. Res.* **15**:698–705 (1998). DOI 10.1023/A:1011910801212.
31. W. L. Chiou, H. Y. Jeong, S. M. Chung, and T. C. Wu. Evaluation of using dog as an animal model to study the fraction of oral dose absorbed of 43 drugs in humans. *Pharm. Res.* **17**:135–140 (2000). DOI 10.1023/A:1007552927404.